ACS Catalysis

Research Article

pubs.acs.org/acscatalysis

Evaluation of the Mechanism of Heterogeneous Hydrogenation of α,β-Unsaturated Carbonyl Compounds via Pairwise Hydrogen Addition

Oleg G. Salnikov,[†,‡] Kirill V. Kovtunov,*[,†,‡] Danila A. Barskiy,[†,‡] Alexander K. Khudorozhkov,[‡,§] Elizaveta A. Inozemtseva,[‡,§] Igor P. Prosvirin,[§] Valery I. Bukhtiyarov,[‡,§] and Igor V. Koptyug[†,‡]

[†]International Tomography Center, SB RAS, 3A Institutskaya St., Novosibirsk 630090, Russia

[‡]Novosibirsk State University, 2 Pirogova St., Novosibirsk 630090, Russia

[§]Boreskov Institute of Catalysis, SB RAS, 5 Acad. Lavrentiev Pr., Novosibirsk 630090, Russia

Supporting Information

ABSTRACT: Heterogeneous hydrogenation of α,β-unsaturated carbonyl compounds was addressed using the parahydrogen-induced polarization (PHIP) technique. PHIP effects were observed in hydrogenation of C=C bond of acrolein and crotonaldehyde over different supported metal catalysts, demonstrating the existence of a pairwise route of hydrogen addition to the substrate. Hydrogenation of acrolein over Pd−Sn/Al_2O_3, Pd−Sn/TiO_2, Pd−Zn/TiO_2, and Pd/TiO_2 catalysts with parahydrogen also led to the polarization of the proton of CHO group of propanal. This was explained by C(O)−H bond dissociation which represents a side process on the catalyst surface. Formation of polarized cis- and trans-2-butenes was detected in hydrogenation of acrolein with parahydrogen over several Rh-based catalysts. This observation is made possible only due to the high NMR signal enhancement provided by PHIP. It was also found that hydrogenation of acetone and propanal with parahydrogen leads to polarized propane formation as a result of C−O bond hydrogenolysis.

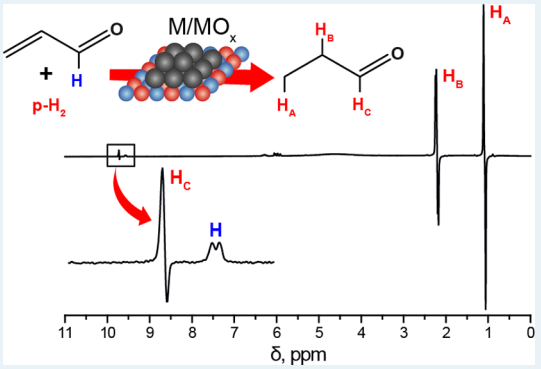

KEYWORDS: *parahydrogen-induced polarization (PHIP), heterogeneous hydrogenation, α,β-unsaturated carbonyl compounds, reaction mechanism, pairwise hydrogen addition*

INTRODUCTION

Selective hydrogenation of unsaturated carbonyl compounds is an industrially important reaction which is widely used in production of pharmaceuticals, flavorings, and perfumes. In most cases, the C=C bonds in such compounds are more readily hydrogenated than the C=O bonds.[1−5] Therefore, selective hydrogenation of the C=O bond in the presence of a C=C bond is a challenging task. It remains an important problem in catalysis, and a lot of efforts are concentrated on research in this field.[2−5] Selective reduction of a C=O bond is a common reaction in fine organic synthesis. Metal hydrides such as $NaBH_4$ and $LiAlH_4$ are usually used as reducing agents. However, these reagents are not appropriate for industrial processes as they are expensive, require rather complicated after-treatments, and sometimes do not provide sufficient selectivity.[6] Another possibility for C=O bond reduction is the Meerwein−Ponndorf−Verley process which is highly selective toward production of alcohols.[7] However, its use in industrial applications also encounters several problems such as poor activity of the catalyst (aluminum isopropoxide) and production of large amounts of waste. Therefore, selective hydrogenation of a C=O bond using heterogeneous catalytic processes is by far preferable for chemical industry. It is notable that selective hydrogenation of unsaturated ketones to unsaturated alcohols is hardly possible because in this case the rate of C=C bond hydrogenation is much higher than that of the C=O bond.[3] Therefore, practically all such studies address hydrogenation of unsaturated aldehydes.

In general, three major products can be formed upon hydrogenation of an α,β-unsaturated aldehyde: saturated aldehyde, unsaturated alcohol (which can isomerize to saturated aldehyde), and saturated alcohol (Figure 1). In addition, hydrocarbons can be produced as byproducts via decarbonylation and C−O bond hydrogenolysis.[3,8,9] Reaction selectivity is affected by many different factors including the nature of the catalyst, the structure of the substrate, and reaction conditions.[3,10] Nowadays, selective hydrogenation catalysts commonly are supported metal nanoparticles. Different metals can be used as an active component, and the selectivity to unsaturated alcohol formation is known to

Received: March 31, 2014
Revised: May 13, 2014
Published: May 13, 2014

   dx.doi.org/10.1021/cs500426a | ACS Catal. 2014, 4, 2022−2028

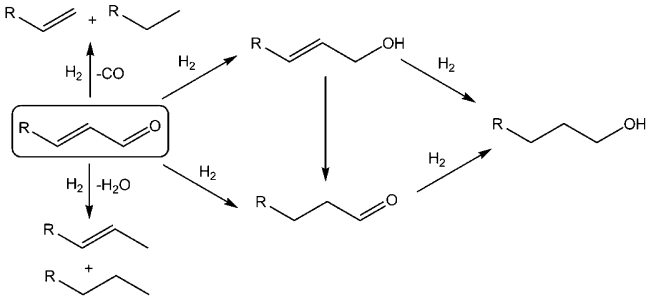

Figure 1. Scheme of possible reaction pathways of α,β-unsaturated aldehydes hydrogenation.

decrease in the sequence Os > Ir > Pt > Ru > Rh > Pd.[3,10] Bimetallic catalysts in which one of these metals is combined with a more electropositive metal such as Sn, Ge, Fe, Co, Ni, Zn, and Mn demonstrate higher selectivity of C=O bond hydrogenation.[3,10] Another possibility to enhance selectivity is to increase the metal particles size.[3,4,10,11] The nature of the support also has an important influence on the selectivity toward C=O bond hydrogenation.[3,4] High-temperature treatment of metal particles supported on reducible oxides such as TiO_2 or Nb_2O_5 in a hydrogen atmosphere leads to formation of TiO_x and NbO_x species which may migrate onto the metal surface. This effect, called SMSI (strong metal−support interaction),[12,13] as well as the use of electron-donating supports (e.g., graphite) increase the selectivity toward formation of unsaturated alcohols.[2−4,10] The substrate structure is also important; for instance, an alkyl substituent at the C=C bond leads to a steric hindrance which destabilizes adsorption via the C=C bond, making adsorption via the C=O bond and therefore its hydrogenation preferable.[3,10] The situation is further complicated by the fact that the mechanism of the reaction is not fully established. Therefore, better understanding and control of the factors which impact the selectivity of the catalytic systems require further studies of the reaction mechanism.

Parahydrogen-induced polarization (PHIP) is an efficient tool for the studies of mechanisms of multiple C−C bond hydrogenation with H_2.[14−18] It provides significant NMR signal enhancements if addition of the parahydrogen (p-H_2) molecule is molecular, or pairwise, i.e., if both ^{1}H nuclei of p-H_2 end up in the same product molecule. High sensitivity and unconventional NMR signal patterns provided by PHIP allow one to study the mechanisms of the catalytic hydrogenations and observe unstable intermediates at low concentrations by detecting the pairwise p-H_2 addition. PHIP was originally considered exclusively in homogeneous reactions catalyzed by transition metal complexes. However, it was proven recently that PHIP effects are also detectable in heterogeneous hydrogenations[19] catalyzed by supported metal nanoparticles,[20−22] immobilized metal complexes,[23] bulk metals, metal oxides,[24] and noble metal-containing zeolite catalysts.[25] Therefore, the PHIP technique can be applied to study the mechanisms of heterogeneous catalytic processes.

In addition to mechanistic studies in catalysis, significant NMR signal enhancement is very important for applications of the MRI technique.[26−29] Substantial progress has been made in this field based on PHIP produced in homogeneous hydrogenations. However, polarized products intended for use as contrast agents must be both catalyst-free and safe for *in vivo* administration. Therefore, further progress with PHIP in heterogeneous reactions can be beneficial for modern biomedical MRI as well.

Practically all heterogeneous PHIP studies reported to date addressed hydrogenation of multiple C−C bonds in unsaturated hydrocarbons,[19] with the only exceptions being the hydrogenation of the C≡C bond in methyl propiolate ($HC{\equiv}C{-}C(O)OCH_3$)[30] and of the C=C bond in acrylamide ($CH_2{=}CH{-}C(O)NH_2$).[31] It would be highly desirable to extend such studies to a much broader variety of substrates to facilitate the production of biocompatible hyperpolarized contrast agents as well as to aid in the investigation of the mechanisms of a much broader range of important catalytic reactions. To this end, we have chosen heterogeneous gas-phase catalytic hydrogenation of α,β-unsaturated carbonyl compounds, acrolein and crotonaldehyde. This choice makes it possible to explore the feasibility of pairwise hydrogenation of the C=O bond, to compare the results with those for the C=C bond hydrogenation, and in addition to produce oxygen-containing products which would be more suitable for bioMRI applications as compared to hydrocarbons. In addition, hydrogenation of α,β-unsaturated carbonyl compounds is known to be accompanied by C−O bond hydrogenolysis, and thus such studies could address the feasibility of extending the PHIP technique to more complex catalytic processes. Hydrogenation of saturated carbonyl compounds such as acetone and propanal was addressed as well in order to further study the selectivity toward alcohols formation and the feasibility of PHIP by pairwise hydrogen addition to the C=O bond. The purpose of this work is thus to extend PHIP studies toward a potentially much broader range of processes and products while not, at this initial stage, going too far from the hydrogenations of multiple C−C bonds that are known to produce PHIP effects.

EXPERIMENTAL SECTION

Catalysts Preparation and Characterization. Commercially available rhodium(III) chloride was used as the precursor for the preparation of rhodium catalysts. Rh(III) oxide was prepared by thermal decomposition of $RhCl_3{\cdot}3H_2O$ at 800 °C for 2 h. The powder was then washed with hot water until the filtrate gave a negative reaction when tested for chloride ions ($AgNO_3 + Cl^- = AgCl + NO_3^-$). Rh black was prepared by a slow reduction of $RhCl_3{\cdot}3H_2O$ aqueous solution with sodium formate at 80 °C. The obtained black precipitate was filtered and washed with hot water until the filtrate gave a negative reaction when tested for chloride ions. Rhodium(III) hydroxide $Rh(OH)_3$ was prepared from $RhCl_3{\cdot}3H_2O$ solution by the addition of sodium hydroxide at 80 °C until pH 10 was reached. The obtained yellowish precipitate was filtered and washed. Rhodium(III) nitrate solution (concentration ∼10 wt %) used as a direct precursor for supported Rh catalysts preparation was obtained by dissolution of $Rh(OH)_3$ in nitric acid (density 1.35 g/mL) with subsequent dilution by a required amount of water. All supported rhodium catalysts contained ∼1% Rh by weight. Palladium(II) nitrate solution with 10.5 wt % palladium concentration was used for supported palladium catalysts preparation. All supported palladium catalysts contained ∼0.9% Pd by weight. In the case of supported platinum catalysts, platinic acid $H_2[Pt(OH)_6]$ was prepared via premixing of $H_2PtCl_6 \times 6H_2O$ aqueous solution with sodium hydroxide with concentrations $[OH^-]/Pt$ = 12:1 at 80 °C for 6 h until pH 13 was reached. The resulting yellowish precipitate was filtered and washed with significant

dx.doi.org/10.1021/cs500426a | *ACS Catal.* 2014, 4, 2022−2028

amounts of glacial acetic acid up to pH 4.5 until the filtrate gave a negative reaction when tested for chloride ions. Platinum(IV) nitrate solution was obtained by dissolution of a weighed amount of $H_2[Pt(OH)_6]$ in nitric acid (density 1.35 g/mL) and subsequent dilution of resulting solution with water until the 20 wt % Pt concentration was reached. All supported platinum catalysts contained ~0.8% Pt by weight.

Metal acetates $M_x(CH_3CO_2)_y{\cdot}zH_2O$ (M = Pd^{2+}, Mn^{3+}, Pb^{2+}, Zn^{2+}, Ag^{+}) from Sigma-Aldrich and $Au(CH_3CO_2)_3$ (Alfa Aesar) were used as precursors for the production of supported bimetallic catalysts. The supports, γ-Al_2O_3 (Sasol, S_{BET} = 215 m^2/g), TiO_2 (Hombifine, S_{BET} = 70 m^2/g), ZrO_2 (TSP, Ekaterinburg, Russia, S_{BET} = 100 m^2/g), and SiO_2 (Sigma-Aldrich, S_{BET} = 350 m^2/g), were ground to powder, calcined at 500 °C for 5 h, and dried at 120 °C for 2 h. Palladium(II) nitrate, platinum(IV) nitrate, and rhodium(III) nitrate were used as precursors for the preparation of supported monometallic catalysts. Bimetallic acetic salts $Pd_xM_y(OAc)_z$ (M = Pb^{2+}, Zn^{2+}, Mn^{3+}, Sn^{2+}, Ag^{+}, Au^{3+}) used for the preparation of bimetallic catalysts were prepared according to the technique proposed by Akhmadullina et al.[32] Catalyst samples were prepared by wet impregnation of supports with corresponding liquid precursor with subsequent drying at 120 °C for 3 h and calcination at 400 °C for 4 h. Then all supported metal catalysts were reduced in hydrogen at 300 °C for 3 h. As a result, bimetallic supported metal catalysts $PdSn/Al_2O_3$ (Pd ~ 1.0%, Sn ~ 0.9%), $PdSn/TiO_2$ (Pd ~ 1.0%, Sn ~ 0.9%), $PdZn/Al_2O_3$ (Pd ~ 1.0%, Zn ~ 1.6%), $PdZn/TiO_2$ (Pd ~ 1.0%, Zn ~ 1.6%), $PdPb/Al_2O_3$ (Pd ~ 1.0%, Pb ~ 0.5%), $PdPb/TiO_2$ (Pd ~ 1.0%, Pb ~ 0.5%), $PdAg/Al_2O_3$ (Pd ~ 0.9%, Ag ~ 0.9%), $PdAu/Al_2O_3$ (Pd ~ 0.9%, Au ~ 1.7%), and $PdMn^{3+}/Al_2O_3$ (Pd ~ 0.9;Mn ~ 0.5) were obtained.

All supported metal catalysts were studied with the XPS technique by recording photoelectron spectra using SPECS spectrometer with PHOIBOS-150-MCD-9 hemispherical energy analyzer (Al Kα, irradiation, $h\nu$ = 1486.6 eV, 200 W). The samples were supported onto double-sided conducting copper Scotch tape. The binding energy (BE) scale was preliminarily calibrated by the position of the peaks of Au $4f_{7/2}$ (BE = 84.0 eV) and Cu $2p_{3/2}$ (BE = 932.67 eV) core levels. The binding energy of peaks was calibrated by the position of the C 1s peak (BE = 284.8 eV) corresponding to the surface hydrocarbon-like deposits (C−C and C−H bonds). Survey spectra were recorded at a pass energy of the analyzer of 50 eV and the narrow spectral regions at 20 eV. Rh and Pd foils, and also PdO and Rh_2O_3 powders, were used as reference materials.

Figure S1(a) presents Pd 3d core-level spectra obtained for Pd−Pb/TiO_2 and Pd−Sn/TiO_2 catalysts. The Pd $3d_{5/2}$ peak at 335.3 eV can be attributed to metallic Pd.[33] Figure S1(b) presents Pd 3d core-level spectra obtained for Pd−Zn/TiO_2 and Pd−Au/Al_2O_3 catalysts, with Pd foil and PdO used as references. For correct identification of the palladium chemical state in the studied samples, we performed curve-fitting for Pd 3d spectra using XPS Peak 4.1 software.[34] The Pd $3d_{5/2}$ peak at 335.2 eV can be attributed to metallic Pd (Pd^0), while the peak at 336.7 eV to Pd^{2+} (PdO).[33] Figure S1(c) presents Pd 3d core-level spectra obtained for Pd/TiO_2 and Pd−Ag/Al_2O_3 catalysts. The Pd $3d_{5/2}$ peak at 336.7 eV can be attributed to Pd^{2+} (PdO).[33] Figure S2 presents Rh $3d_{5/2}$ core-level spectra obtained for the Rh/TiO_2 catalyst and rhodium foil and Rh_2O_3 as the references. The Rh $3d_{5/2}$ peak at 308.2 eV can be attributed to metallic Rh (Rh^0) and the peak at 308.7 eV to Rh^{3+} (Rh_2O_3).[33]

Hydrogenation Reactions and NMR Experiments. All hydrogenation experiments were carried out using commercially available acrolein (Fluka, >95%), crotonaldehyde (Sigma-Aldrich, >99.5%), acetone, propanal, and hydrogen. For PHIP experiments, H_2 was enriched with parahydrogen up to 50% by passing it through FeO(OH) (Sigma-Aldrich) powder maintained at liquid nitrogen temperature.[20] After the enrichment stage, hydrogen was collected in a gas cylinder. During the experiments, it was bubbled through the flask containing liquid substrate (acrolein, crotonaldehyde, acetone, or propanal). In the case of PASADENA[14] experiments (hydrogenation in the high magnetic field of the NMR spectrometer), the mixture of hydrogen and the substrate vapor was supplied through a Teflon capillary to the bottom of a 10 mm NMR tube where the catalyst was placed. For ALTADENA[15] experiments (hydrogenation in Earth's magnetic field with subsequent transfer of reaction products to the NMR spectrometer for analysis), the mixture of H_2 and the substrate vapor was supplied to the reactor comprising a straight piece of a copper tube with the catalyst packed between two pieces of fiberglass tissue, and then to an empty NMR tube. In all experiments, the NMR tube residing in the NMR instrument was heated to 100−130 °C to prevent condensation of the reaction products and, in the case of PASADENA experiments, to initiate the *in situ* hydrogenation. In ALTADENA experiments, the copper reactor was heated with an electric tubular furnace. All hydrogenations were carried out at atmospheric pressure. The gas flow rate (from ~1 to ~17 mL/s) was measured with a rotameter. The experimental conditions such as the catalyst mass and the reactor temperature are summarized in the Supporting Information SI (Table S1 in the SI). The experimental setup is also presented schematically in SI (Figure S3). For the liquid phase hydrogenation, the mixture with a H_2/acrolein vapor ratio of 8:1 was prepared in a gas cylinder and supplied to the NMR tube containing 0.03 g of Pd/TiO_2 catalyst and approximately 5 mL of d_8-toluene. NMR spectra were recorded immediately after stopping the gas flow. ^{1}H NMR spectra were recorded on a 300 MHz Bruker AV 300 NMR spectrometer. The 45° (PASADENA) and 90° (ALTADENA) radiofrequency pulses were used for the NMR signal detection.

RESULTS AND DISCUSSION

Acrolein was hydrogenated with p-H_2 over several different supported Pd- and Pt-based catalysts (Pt/Al_2O_3, Pt/SiO_2, Pt/C, Pd/Al_2O_3, Pd/SiO_2, Pd/TiO_2, Pd−Sn/Al_2O_3, Pd−Sn/TiO_2, Pd−Zn/Al_2O_3, Pd−Zn/TiO_2, Pd−Pb/Al_2O_3, Pd−Pb/TiO_2, Pd−Ag/Al_2O_3, Pd−Au/Al_2O_3, Pd−Mn^{3+}/Al_2O_3, Pt−Y−Ce−Zr/Al_2O_3) using the PASADENA[14] technique. In all cases, the polarized NMR signals of CH_3 and CH_2 protons of propanal were observed, with some representative examples shown in Figure 2. The Pd−Sn/Al_2O_3 catalyst was also tested in ALTADENA[15] experiments, and the same NMR signals exhibited polarization (see Figure S4). The observation of PHIP effects shows that H_2 addition upon hydrogenation of the C═C bond of acrolein can be pairwise. It is notable that the intensities of PHIP patterns were much higher for the Pd-based catalysts than for the Pt-based catalysts. The main reason is the higher activity of the former in hydrogenation of the C═C bond of α,β-unsaturated carbonyl compounds, which is expected from both experimental and theoretical research.[3,10] Moreover, in the case of supported palladium catalysts, Pd^{2+} and Pd^0 show similar activities in terms of the pairwise

dx.doi.org/10.1021/cs500426a | ACS Catal. 2014, 4, 2022−2028

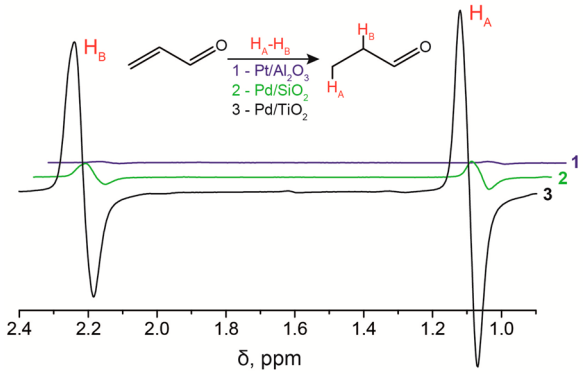

Figure 2. ^{1}H NMR PASADENA spectra of CH_3 and CH_2 protons of propanal recorded *in situ* during hydrogenation of acrolein over Pt/Al_2O_3, Pd/SiO_2, and Pd/TiO_2 catalysts.

hydrogen addition, which may be explained by reduction of Pd^{2+} to Pd^0 during the highly exothermic hydrogenation processes (Figure S1 in the SI). The hydrogenation of the C═O bond is hardly possible with many catalysts, and only for Pd/Al_2O_3, Pd/TiO_2, and Pd−Zn/TiO_2 catalysts the low-intensity nonpolarized NMR signals of propanol were detected. Interestingly, in the case of Pd−Sn/Al_2O_3, Pd−Sn/TiO_2, Pd−Zn/TiO_2, and Pd/TiO_2 catalysts, in addition to the CH_3 and CH_2 protons, the proton of the CHO group of propanal exhibited the PHIP effect (Figure 3b). A possible mechanism which can lead to polarization of the CHO proton is presented in Figure 3a. The crucial step is the formation of surface Pd−C(O)−CH═CH_2 species which are hydrogenated with p-H_2 via the pairwise route. The observation of Pt−C(O)CH_3 intermediates in ethanol adsorption on Pt has been reported.[35] Moreover, the formation of Ti−O═C−CH_3 species was theoretically predicted in acetaldehyde adsorption on TiO_2.[36] Therefore, we assume that the C(O)−H bond can be broken on the metal as well as on the support surface as shown in Figure 3a. Moreover, in this case, the hydrogenation reaction can proceed on the interface between the metal and the support.[37] The process leading to CHO-proton polarization is the minor route of the reaction, but strong signal enhancement which is produced by PHIP allows us to detect it.

For the Rh-based catalysts, the performance was significantly different from that of Pd- and Pt-based catalysts. In the case of ALTADENA experiments with Rh/Al_2O_3 catalyst and PASADENA experiments with Rh/Al_2O_3, Rh/TiO_2, Rh_2O_3, and bulk Rh metal catalysts, in addition to the polarized propanal signals, two other strongly polarized NMR signals were observed at 5.5 and 1.6 ppm (Figure 4). The chemical shifts along with the absence of any additional polarized lines in the spectra imply the formation of a mixture of cis- and trans-2-butenes. From the equilibrium NMR spectra, their yield was estimated as <4%. For an additional direct verification of 2-butene formation in these experiments, we compared the PASADENA experiment for acrolein with that for 2-butyne. It was shown that the shapes of PASADENA-polarized lines and their positions (5.5 and 1.6 ppm) in the ^{1}H NMR spectra are the same for the two experiments (Figure S5 in the SI), confirming beyond a doubt that 2-butenes are formed in both cases.

It is well-known that supported Rh nanoparticles are able to decarbonylate aldehydes.[38,39] In the case of unsaturated aldehyde, acrolein, breaking of the C−C(O) bond should

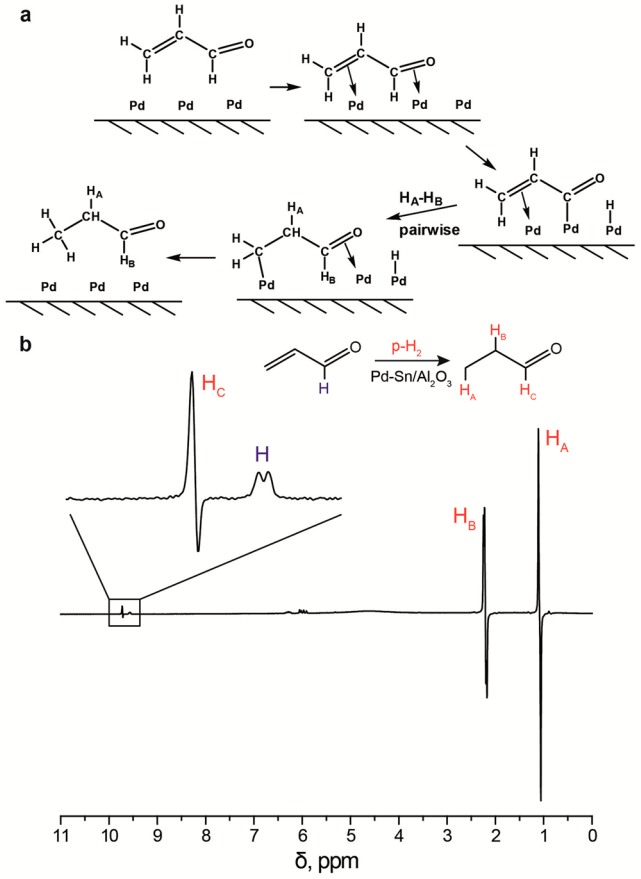

Figure 3. Proposed reaction mechanism which explains the observation of polarization on the CHO proton of propanal (a) and ^{1}H NMR spectrum acquired in hydrogenation of acrolein with p-H_2 over Pd−Sn/Al_2O_3 (b).

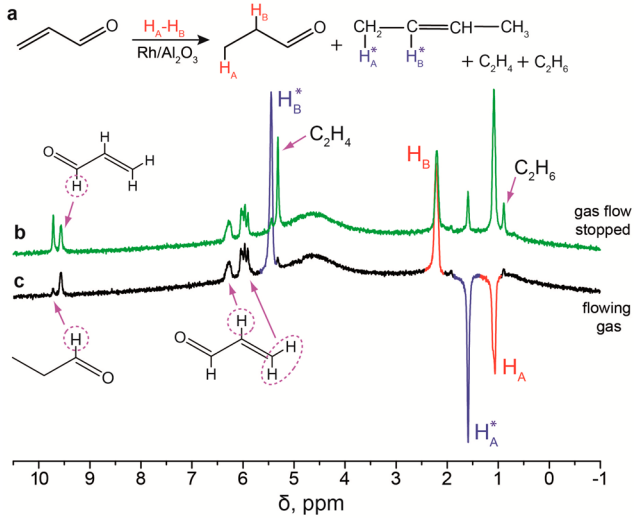

Figure 4. Scheme of acrolein hydrogenation over Rh/Al_2O_3 (a). ^{1}H NMR ALTADENA spectra acquired during hydrogenation of acrolein over Rh/Al_2O_3 with gas flow stopped (b) and with flowing gas (c).

release a vinyl species CH_2═CH. Other conceivable leaving groups that may be formed at the Rh surface include those with a larger number of hydrogen atoms, e.g., C_2H_5, CH_3CH or CH_2═CH_2, an isomer of the vinyl CH_3C, and CH_2C or HC≡CH.[39] Moreover, Barteau and Brown reported that vinyl and

dx.doi.org/10.1021/cs500426a | *ACS Catal.* 2014, 4, 2022−2028

acetylene are the most likely candidates for ligands that are eliminated in acrolein decarbonylation.[39] However, adsorbed acetylene undergoes hydrogenation to ethylene and ethylidyne species on the Rh surface.[40] The formation of ethylene and ethane in acrolein hydrogenation was successfully detected in our experiments with several heterogeneous catalysts including the Rh-based ones (Rh/Al_2O_3, Rh_2O_3, Rh, Pd/Al_2O_3, Pt/Al_2O_3, $Pd–Sn/Al_2O_3$, $Pd–Sn/TiO_2$, Pd/TiO_2, $Pd–Ag/Al_2O_3$, $Pd–Au/Al_2O_3$, $Pd–Zn/TiO_2$; Figure 4). Therefore, one of the plausible explanations of polarized 2-butene formation during acrolein hydrogenation over Rh nanoparticles is the oligomerization of vinyl species with subsequent addition of p-H_2 in a pairwise manner. While 2-butenes are minor products of the reaction, the strong signal enhancement allows one to observe their formation. Our observations once again confirm the fact that PHIP is a very informative method for studying the mechanisms of both major and minor routes of hydrogenation reactions. The observation of PHIP effects in reaction products in many cases can provide valuable information about the mechanism even if the structures of intermediates are not known, as in our experiments with 2-butene formation during acrolein hydrogenation.

Next, liquid phase heterogeneous hydrogenation of acrolein was performed by bubbling p-H_2 through the solution of acrolein in toluene-d_8 in the presence of the solid catalyst, and the pairwise hydrogen addition to the C═C bond could be detected, similar to the gas-phase experiments. In PASADENA experiments with the Pd/TiO_2 catalyst, we observed polarized NMR signals of CH_3 and CH_2 groups of propanal (see Figure S6 in the SI). However, intensities of the polarized lines were lower than for gas-phase hydrogenation due to the low activity of the catalyst in the liquid phase.

For more substituted carbonyl compounds, the selectivity toward C═O bond hydrogenation is known to be higher.[3,10] Therefore, in order to observe C═O bond hydrogenation, such compounds as crotonaldehyde, prenal (3-methylbut-2-enal), and cinnamaldehyde can be more suitable than acrolein. For prenal and cinnamaldehyde, only liquid-phase experiments can be efficiently performed because of their low volatility. Therefore, crotonaldehyde was used next as a substrate for hydrogenation in the gas phase over Pt/Al_2O_3, Pt/TiO_2, Pt/SiO_2, Pt/ZrO_2, Pd/TiO_2, Pd/SiO_2, Pd/ZrO_2, Rh/Al_2O_3, Rh/TiO_2, $Pd–Sn/Al_2O_3$, and $Pd–Sn/TiO_2$ catalysts using the PASADENA protocol. Polarized NMR signals of CH_2 groups of butanal were observed in all cases. This, without a doubt, confirms the existence of a reaction pathway where the C═C double bond may add hydrogen molecularly and, importantly, with the preservation of the spin coherence of two protons originating from the same p-H_2 molecule. Importantly, when Pd/TiO_2, Pd/ZrO_2, and $Pd–Sn/Al_2O_3$ catalysts were used for crotonaldehyde gas-phase heterogeneous hydrogenation, not only the C═C but also the C═O bond was hydrogenated (Figure 5). It should be noted that the C═O bond reacts only after the C═C bond hydrogenation because only signals of butanal and butanol, but not but-2-en-1-ol, were observed in the ^{1}H NMR spectra. Moreover, butanol is formed in significant quantities only at the low flow rates of a gas mixture through the catalyst layer when conversion is sufficiently high. However, slow gas flow makes it difficult to observe PHIP effects because of the relatively fast relaxation of polarization (Figure 5b). When the gas is flowing (17 mL/s), the ^{1}H NMR signals of butanol are not detected (Figure 5c). However, in the case of Pt/Al_2O_3, Pt/TiO_2, Pt/SiO_2, Pd/TiO_2, Rh/TiO_2, and $Pd–Sn/TiO_2$ catalysts, the polarized NMR signals of propane were observed. Propane is formed as a result of decarbonylation, which is a common side process in the hydrogenation of aldehydes on metals.[3,8,37]

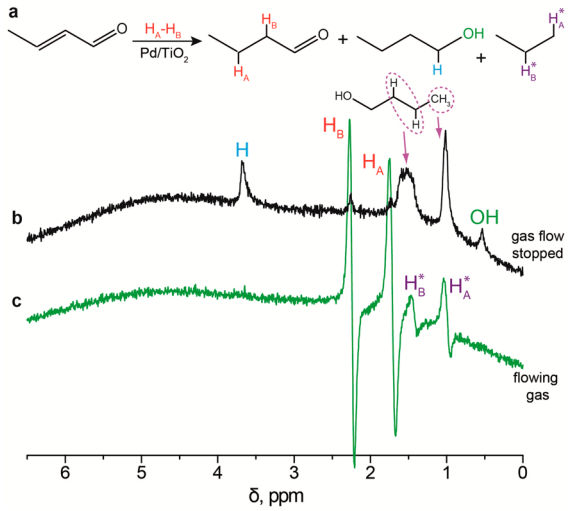

Figure 5. Scheme of crotonaldehyde hydrogenation over Pd/TiO_2 (a). ^{1}H NMR PASADENA spectra acquired during hydrogenation of crotonaldehyde over Pd/TiO_2 with gas flow stopped (b) and with flowing gas (c).

In our experiments with acrolein and crotonaldehyde, only protons added to C═C bonds were polarized. Therefore, substrates possessing only the C═O but not the C═C group were used in the next attempts. Heterogeneous hydrogenation of acetone vapor over Pt/Al_2O_3, Pt/TiO_2, Pd/Al_2O_3, Pd/TiO_2, Rh/TiO_2, Rh/SiO_2, and $Pd–Sn/Al_2O_3$ catalysts yielded isopropanol, but in all cases its ^{1}H NMR signals did not exhibit any PHIP effects. At the same time, the Rh/TiO_2 and Rh/Al_2O_3 catalysts in addition produced polarized propane (Figure S7). A similar situation was observed for propanal hydrogenation catalyzed by Pt/TiO_2 and Pd/TiO_2. Propanol and propane were formed in the reaction, while PHIP was observed only for the CH_3 and CH_2 groups of propane (Figure S8). Propane could be produced from the corresponding alcohol (isopropanol or propanol) by dehydration/hydrogenation processes. In this case, hydrogenation of propanol with p-H_2 under the same conditions should lead to PHIP observation. However, when propanol was used in heterogeneous hydrogenation with p-H_2, no reaction products were detected. Thus, propane is formed directly from the carbonyl compounds, most probably as a result of C–O bond hydrogenolysis.

The fact that PHIP effects corresponding to pairwise hydrogen addition to C═O bond of unsaturated and saturated aldehydes were not observed could be the result of a specific reaction mechanism. In a recent publication of Kennedy et al.,[37] the authors studied hydrogenation of crotonaldehyde, crotyl alcohol, and butanal over Pt/TiO_2 and Pt/SiO_2 catalysts using *in situ* sum-frequency generation vibrational spectroscopy. They concluded that in the case of the Pt/TiO_2 catalyst, the C═O bond is hydrogenated by H atoms spilled over from the metal to the support, whereas for the Pt/SiO_2 catalyst this reaction pathway is hardly possible due to the inert nature of the SiO_2 support. We attempted to hydrogenate propanal with p-H_2 using Pt/TiO_2 and Pt/SiO_2 as the catalysts. No hyperpolarization of reaction products was observed in these

dx.doi.org/10.1021/cs500426a | *ACS Catal.* 2014, 4, 2022–2028

experiments. In the case of Pt/TiO_2, this could be the result of participation of spillover hydrogen in the reaction[37] because incorporation of random H atoms is not expected to produce any PHIP effects. The activity of the Pt/SiO_2 catalyst was significantly lower than that of Pt/TiO_2: no reaction was observed at 120 °C; at 150 °C (in ALTADENA conditions) decarbonylation leading to ethane began, and only at 300 °C did the hydrogenation become apparent, but without any PHIP effects.

CONCLUSION

Parahydrogen-induced polarization (PHIP) was used for studying the heterogeneous hydrogenation of several unsaturated (acrolein, crotonaldehyde) and saturated (acetone, propanal) carbonyl compounds. PHIP effects were successfully observed in liquid and gas phase hydrogenations of the C=C bond of acrolein and crotonaldehyde over several supported metal catalysts. These observations confirm the existence of the route of pairwise hydrogen addition to the C=C bond of unsaturated aldehydes in the reaction mechanism. At the same time, no PHIP effects that would correspond to pairwise hydrogen addition to the C=O bond could be observed for unsaturated and saturated substrates tested. However, the conversion to alcohols was very low in all cases. Therefore, to address the feasibility of PHIP observation in C=O bond hydrogenation it would be valuable to come up with catalytic systems and reaction conditions that provide a much higher activity in this reaction. Upon hydrogenation of acrolein over several of the supported metal catalysts, the NMR signal of the CHO group of propanal was also polarized, possibly as a result of a minor process in which the C(O)−H bond is broken. Furthermore, the formation of polarized cis- and trans-2-butenes was detected in hydrogenation of acrolein over several Rh-based catalysts, and polarized propane was formed in heterogeneous hydrogenation of acetone and propanal as a result of C−O bond hydrogenolysis. This demonstrates that the applicability of PHIP can be successfully extended from hydrogenations to other more complex catalytic reactions, which generally improves the availability of PHIP as the technique for uncovering fine details of catalytic processes including identification of the structure and the mechanism of formation of less abundant reaction products.

ASSOCIATED CONTENT

Supporting Information

Catalysts used, experimental setup and conditions, and additional NMR spectra. This material is available free of charge via the Internet at http://pubs.acs.org.

AUTHOR INFORMATION

Corresponding Author

*E-mail: kovtunov@tomo.nsc.ru.

Notes

The authors declare no competing financial interest.

ACKNOWLEDGMENTS

This work was partially supported by the RAS (5.1.1), RFBR (12-03-00403-a, 14-03-00374-a, 14-03-31239-mol-a), SB RAS (60, 61), the Ministry of Education and Science of the Russian Federation, and the Council on Grants of the President of the Russian Federation (MK-4391.2013.3).

REFERENCES

(1) Narayanan, S. *Bull. Catal. Soc. Ind.* **2003**, *2*, 107−121.
(2) Claus, P. *Top. Catal.* **1998**, *5*, 51−62.
(3) Gallezot, P.; Richard, D. *Catal. Rev.: Sci. Eng.* **1998**, *40*, 81−126.
(4) Mäki-Arvela, P.; Hájek, J.; Salmi, T.; Murzin, D. Yu. *Appl. Catal., A* **2005**, *292*, 1−49.
(5) Ponec, V. *Appl. Catal., A* **1997**, *149*, 27−48.
(6) Daimon, A.; Kamitanaka, T.; Kishida, N.; Matsuda, T.; Harada, T. *J. Supercrit. Fluids* **2006**, *37*, 215−219.
(7) de Graauw, C. F.; Peters, J. A.; van Bekkum, H.; Huskens, J. *Synthesis* **1994**, *10*, 1007−1017.
(8) Touroude, R. *J. Catal.* **1980**, *65*, 110−120.
(9) Birchem, T.; Pradier, C. M.; Berthier, Y.; Cordier, G. *J. Catal.* **1994**, *146*, 503−510.
(10) Delbecq, F.; Sautet, P. *J. Catal.* **1995**, *152*, 217−236.
(11) Wei, H.; Gomez, C.; Liu, J.; Guo, N.; Wu, T.; Lobo-Lapidus, R.; Marshall, C. L.; Miller, J. T.; Meyer, R. J. *J. Catal.* **2013**, *298*, 18−26.
(12) Tauster, S. J.; Fung, S. C.; Garten, R. L. *J. Am. Chem. Soc.* **1978**, *100*, 170−175.
(13) Tauster, S. J. *Acc. Chem. Res.* **1987**, *20*, 389−394.
(14) Bowers, C. R.; Weitekamp, D. P. *J. Am. Chem. Soc.* **1987**, *109*, 5541−5542.
(15) Pravica, M. G.; Weitekamp, D. P. *Chem. Phys. Lett.* **1988**, *145*, 255−258.
(16) Duckett, S. B.; Mewis, R. E. *Acc. Chem. Res.* **2012**, *45*, 1247−1257.
(17) Natterer, J.; Bargon, J. *Prog. NMR Spectrosc.* **1997**, *31*, 293−315.
(18) Blazina, D.; Duckett, S. B.; Dunne, J. P.; Godard, C. *Dalton Trans.* **2004**, 2601−2609.
(19) Kovtunov, K. V.; Zhivonitko, V. V.; Skovpin, I. V.; Barskiy, D. A.; Koptyug, I. V. In *Topics in Current Chemistry*; Kuhn, L. T., Ed.; Springer-Verlag: Berlin, 2013; Vol. *338*, pp 123−180.
(20) Kovtunov, K.; Beck, I.; Bukhtiyarov, V.; Koptyug, I. *Angew. Chem., Int. Ed.* **2008**, *47*, 1492−1495.
(21) Zhivonitko, V. V.; Kovtunov, K. V.; Beck, I. E.; Ayupov, A. B.; Bukhtiyarov, V. I.; Koptyug, I. V. *J. Phys. Chem. C* **2011**, *115*, 13386−13391.
(22) Kovtunov, K. V.; Beck, I. E.; Zhivonitko, V. V.; Barskiy, D. A.; Bukhtiyarov, V. I.; Koptyug, I. V. *Phys. Chem. Chem. Phys.* **2012**, *14*, 11008−11014.
(23) Koptyug, I. V.; Kovtunov, K. V.; Burt, S. R.; Anwar, M. S.; Hilty, C.; Han, S.; Pines, A.; Sagdeev, R. Z. *J. Am. Chem. Soc.* **2007**, *129*, 5580−5586.
(24) Kovtunov, K. V.; Barskiy, D. A.; Salnikov, O. G.; Khudorozhkov, A. K.; Bukhtiyarov, V. I.; Prosvirin, I. P.; Koptyug, I. V. *Chem. Commun.* **2014**, *50*, 875−878.
(25) Henning, H.; Dyballa, M.; Scheibe, M.; Klemm, E.; Hunger, M. *Chem. Phys. Lett.* **2013**, *555*, 258−262.
(26) Golman, K.; Axelsson, O.; Jóhannesson, H.; Månsson, S.; Olofsson, C.; Petersson, J. S. *Magn. Reson. Med.* **2001**, *46*, 1−5.
(27) Bhattacharya, P.; Harris, K.; Lin, A. P.; Mansson, M.; Norton, V. A.; Perman, W. H.; Weitekamp, D. P.; Ross, B. D. *Magn. Reson. Mater. Phys. Biol. Med.* **2005**, *18*, 245−256.
(28) Reineri, F.; Viale, A.; Giovenzana, G.; Santelia, D.; Dastru, W.; Gobetto, R.; Aime, S. *J. Am. Chem. Soc.* **2008**, *130*, 15047−15053.
(29) Dechent, J. F.; Buljubasich, L.; Schreiber, L. M.; Spiess, H. W.; Münnemann, K. *Phys. Chem. Chem. Phys.* **2012**, *14*, 2346−2352.
(30) Balu, A. M.; Duckett, S. B.; Luque, R. *Dalton Trans.* **2009**, 5074−5076.
(31) Koptyug, I. V.; Zhivonitko, V. V.; Kovtunov, K. V. *ChemPhysChem* **2010**, *11*, 3086−3088.
(32) Akhmadullina, N. S.; Cherkashina, N. V.; Kozitsyna, N. Yu.; Stolarov, I. P.; Perova, E. V.; Gekhman, A. E.; Nefedov, S. E.; Vargaftik, M. N.; Moiseev, I. I. *Inorg. Chim. Acta* **2009**, *362*, 1943−1951.
(33) Moudler, J.; Stickle, W.; Sobol, P.; Bomben, K. *Handbook of X-ray Photoelectron Spectroscopy*; Perkin-Elmer Corp.: Eden Priarie, MN, 1992.
(34) XSPEAK 4.1 Download (Free). http://xpspeak.software.informer.com/4.1/.

(35) Iwasita, T.; Pastor, E. *Electrochim. Acta* **1994**, *39*, 531−537.
(36) Gaba, R.; Bhandari, M.; Kakkar, R. *Adv. Mater. Lett.* **2013**, *4*, 769−778.
(37) Kennedy, G.; Baker, L. R.; Somorjai, G. A. *Angew. Chem., Int. Ed.* **2014**, *53*, 3405−3408.
(38) Houtman, C. J.; Barteau, M. A. *J. Catal.* **1991**, *130*, 528−546.
(39) Brown, N. F.; Barteau, M. A. *J. Am. Chem. Soc.* **1992**, *114*, 4258−4265.
(40) Dubois, L. H.; Castner, D. G.; Somorjai, G. A. *J. Chem. Phys.* **1980**, *72*, 5234−5240.